presently remains dismal, and novel diagnostic and therapeutic modalities, or improvement of existing therapeutic strategies, have long been required to improve the clinical outcome of patients with HCC.

Histological differentiation is a hallmark of malignant potential of HCC; patients with poorly-differentiated tumors tend to have worse prognosis than those with well-differentiated tumors.[6] Therefore, the molecular background of histological differentiation may involve prognostic biomarker candidates, which may lead to novel diagnostic and therapeutic modalities. However, although several factors regulating histological differentiation have been reported,[7,8] proteins that underlie HCC differentiation and correlate with HCC prognosis are presently unclear.

Recently, the advent of novel technologies linked with the Human Genome Database enabled global protein expression studies, namely proteomics.[9] The proteome is the functional translation of the genome, directly regulating cancer behavior, and is thus a rich source for identifying biomarkers and therapeutic targets. Proteomic studies have identified the proteins whose expression correlates with early recurrence of HCC.[10,11] The proteins implicated in early recurrence may have a clinical utility in predicting poor prognosis. Recently, we identified the proteins associated with histological differentiation in esophageal cancer using two-dimensional difference gel electrophoresis (2D-DIGE).[12] As the identified proteins included those associated with malignant attributes of tumor cells such as lymph node metastasis, this approach is also worth being applied to the study of HCC.

We conducted a proteomic study on HCC tissues with varying degrees of histological differentiation, as well as adjacent nontumor tissues and normal liver tissues, and captured a molecular signature that underlies HCC differentiation and affects the malignant potential of HCC. We found that expression of APC-binding protein EB1 (EB1) was specific to moderately-differentiated and poorly-differentiated HCCs, and revealed the prognostic value of EB1 expression, employing immunohistochemistry on additional HCC cases.

Materials and Methods

Detailed procedures are available in the Supporting Information.

Patients and Tissue Samples. A total of 45 surgically resected tissues were included in this study. The tissue samples were divided into five groups according to their histological classification: seven normal liver tissues, 11 nontumor tissues adjacent to tumors, six well-differentiated HCCs, 14 moderately-differentiated HCCs, and seven poorly-differentiated HCCs (Supporting Table 1). The tissues were obtained at the National Cancer Center Hospital; the HCC and adjacent nontumor tissues were from patients with HCC who underwent initial hepatic resection between June 2005 and April 2006, and the normal liver tissues were from patients who underwent hepatic resection for metastatic liver tumor from colorectal cancer in the same period. Different histological areas of HCC were obtained from identical tumor tissues of three cases whose tumors showed histological heterogeneity. The clinicopathological features of the patients are listed in Supporting Table 1. For the EB1 expression study, we examined an additional 145 patients with HCC who underwent initial surgical resection between February 1992 and December 2000 at the National Cancer Center Hospital. None of the patients of this study received any preoperative therapy. Tumors were classified according to the World Health Organization classification[13] and the International Union against Cancer tumor-node-metastasis (TNM) classification.[14] The ethical review board of the National Cancer Center approved this project.

Laser Microdissection. Specific populations of cells were recovered by laser microdissection according to our previous reports[15,16] (Fig. 1A). In brief, 10-μm-thick frozen sections were created from tumor tissues and stained with hematoxylin. The cells were recovered under microscopic observation with the assistance of a ultraviolet laser (MMI CellCut; Molecular Machines & Industries, Glattbrugg, Switzerland). A 1-mm^2 tissue area (~3,000 cells) was recovered for one gel. The recovered cells were lysed in urea lysis buffer containing 6 M urea, 2 M thiourea, 3% {3-[(3-cholamidopropyl)dimethylammonio]-1-propanesulfonate}, and 1% Triton X-100, and were stored at -80°C until use.

2D-DIGE and Image Analysis. The 2D-DIGE was performed as described.[15,16] In brief, a common internal control sample was created by mixing a small portion of all protein samples used in this study, and labeled with cyanine 3 (Cy3) fluorescent dye (CyDye DIGE Fluor saturation dye; GE Healthcare Biosciences, Uppsala, Sweden). Individual samples were labeled with cyanine 5 (Cy5) fluorescent dye (CyDye DIGE Fluor saturation dye; GE Healthcare Biosciences). These differently-labeled protein samples were mixed together and separated according to their isoelectric point and molecular weight. The first dimension separation was achieved using a 24-cm-length immobiline gel (IPG, pI 4-7; GE Healthcare Biosciences) and Multiphor II (GE Healthcare Biosciences), while the second-dimension separation used a homemade gradient gel with GiantGelRunner (Biocraft, Tokyo, Japan), with a separation distance of 36 cm. The gels were scanned using a laser scanner (Typhoon Trio; GE Healthcare Biosciences) at the appropriate wavelength for Cy3 or Cy5. For all protein spots, the Cy5

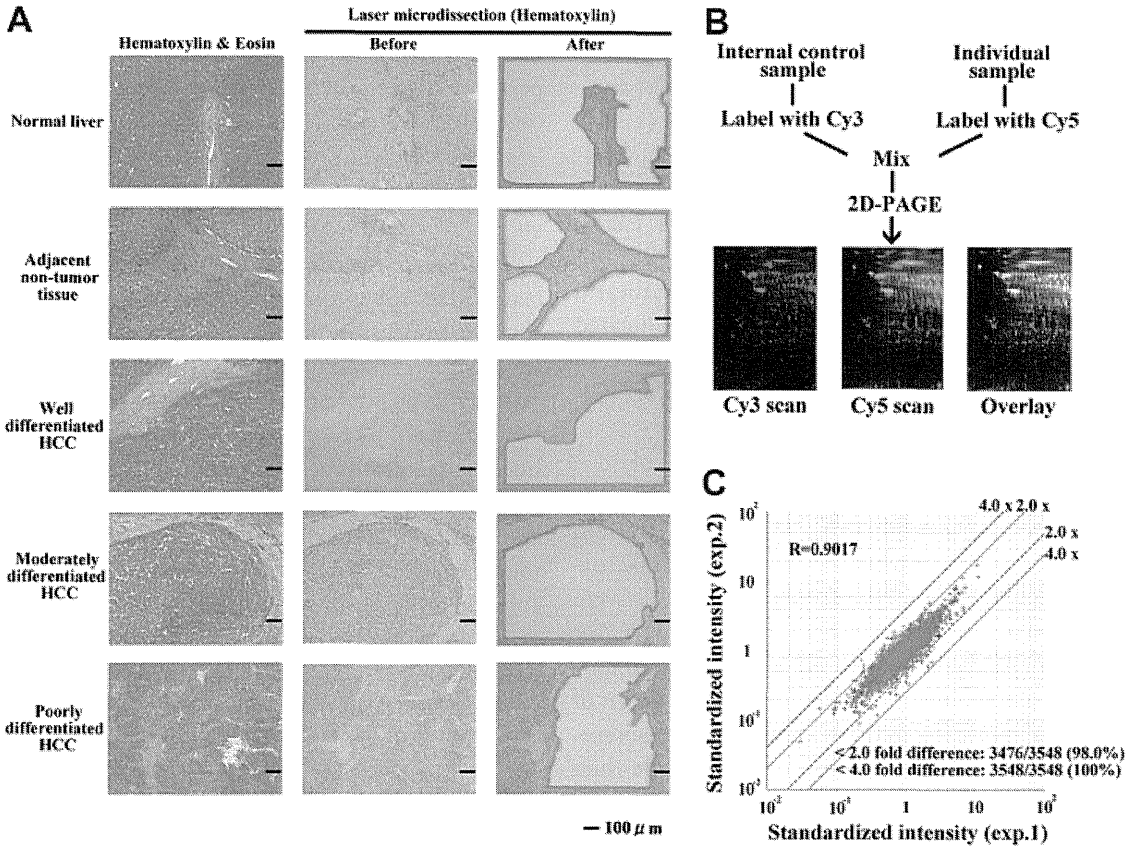

Fig. 1. Protein expression profiling using laser microdissection and 2D-DIGE with high sensitive fluorescent dyes. (A) Specific populations of cells were recovered using laser under microscopic observation. (B) The extracted proteins were labeled with fluorescent dyes and separated by two-dimensional polyacrylamide gel electrophoresis (2D-PAGE). (C) Evaluation of the reproducibility of 2D-DIGE by scatter graphs.

intensity was normalized with the Cy3 intensity in the same gel using the DeCyder software (version 5.0; GE Healthcare Biosciences), so that gel-to-gel variations were canceled out (Fig. 1B). We monitored the reproducibility of our system by running the same sample twice (case 24; Supporting Table 1). The scatter-plot demonstrated that the intensity value of 98% of protein spots was scattered within a two-fold difference, and that the correlation coefficient was 0.9017, showing the high reproducibility of the profiling method used (Fig. 1C). The spot intensity data were exported from the DeCyder software as extensible markup language (XML) format files, which are amenable to data analysis.

Data Analysis. The numerical data in the XML files were imported to Expressionist software (GeneData, Basel, Switzerland) for scatter-plotting, hierarchical clustering, and principal component analysis. The Kruskal-Wallis test and Bonferroni adjustment were used to identify the protein spots that were differentially expressed in the five tissue groups examined.

Mass Spectrometric Protein Identification. The proteins corresponding to the protein spots were identified by mass spectrometry according to our report.[12] Cy5-labeled proteins separated by 2D-polyacrylamide gel electrophoresis (PAGE) were recovered in gel plugs and digested with modified trypsin (Promega, Madison, WI). The trypsin digests were subjected to liquid chromatography, coupled with tandem mass spectrometry equipped with a nanoelectrospray ion source (Paradigm MS4 dual solvent delivery system; Michrom BioResources Inc., Auburn, CA) for microflow high-performance liquid chromatography (HPLC), an HTS PAL auto sampler (CTC Analytics, Zwingen, Switzerland), and a Finnigan LTQ linear ion trap mass spectrometer (ThermoElectron Co., San Jose, CA) equipped with a nanoelectrospray ion source (AMR Inc., Tokyo, Japan). The Mascot software (version 2.1; Matrix Science, London, UK) was used to search for the mass of the peptide ion peaks against the SWISS-PROT database (*Homo sapiens*; 12867 sequence in Sprot_47.8 fasta file). Proteins with a Mascot score of 35 or more were used for protein identification. When multiple proteins were identified in a single spot, the proteins with the highest number of peptides were considered as those corresponding to the spot.

Western Blotting. Protein samples were separated by sodium dodecyl sulfate (SDS)-PAGE and subsequently blotted on a nitrocellulose membrane. Immunoblot analysis was performed using the antibodies EB1 (1:200; Santa Cruz Biotechnology, Santa Cruz, CA), proliferating cell nuclear antigen (1:5,000; BD Transduction Laboratories, San Jose, CA), heat shock protein 90 (1;1,000; BD Transduction Laboratories), arginase-I (1;1,000; BD Transduction Laboratories), actin (1;2;000; Abcam, Cambridge, UK), horseradish peroxidase–conjugated secondary antibodies (1:1,000; GE Healthcare Biosciences), and enhanced chemiluminescence (ECL; GE Healthcare Biosciences).

Immunohistochemistry. Immunohistochemical staining for EB1 was performed on formalin-fixed, paraffin-embedded tissue sections using the CSA II system (DAKO, Glostrup, Denmark) following the manufacturer's instructions. For antigen retrieval, the sections were autoclaved in 10 mM citrate buffer (pH 6.0) at 121°C for 10 minutes. We used rabbit anti-EB1 polyclonal antibodies (sc-15347; Santa Cruz Biotechnology) at a dilution of 1:500. Staining was assessed by two independent observers in a blinded fashion for clinical data. The bile duct epithelium served as an internal control of positive staining. If more than 50% of tumor cells were positively stained, the tumor was judged as EB1-positive. Staining evaluation was done at the dominant differentiation area of the tumor if the tumor had areas with varying degrees of differentiation.

Pathway Analysis of Expression Data. The pathway analysis of the protein expression pattern was performed using the MetaCore software (GeneGo Inc., St. Joseph, MI). MetaCore identifies networks based on a manually curated database containing known molecular interactions, functions, and disease interrelationships, using proteome data sets. The pathways were identified by the probability that a random set of proteins the same size as the input list would give rise to a particular mapping by chance.

Statistical Analysis. The correlation between EB1 expression and clinicopathological features was evaluated by the Fisher exact test for categorical variables and the Mann-Whitney *U* test for continuous variables. The time to recurrence and overall survival were calculated from the first resection of the primary tumor to the first radiological evidence of recurrence or to death, respectively. All time-to-event end points were computed by the Kaplan-Meier method.[17] Patients dying without recurrence were censored in determining recurrence. Potential prognostic factors were identified by univariate analysis using the log-rank test. Independent prognostic factors were evaluated using a Cox proportional hazards regression model and a stepwise selection procedure. P differences <0.05 were considered to be significant. Statistical analyses were performed using the SPSS statistical package (SPSS, Chicago, IL).

Results

Proteomic Profiling of HCC. To examine the overall features of the proteome, we performed unsupervised classification using the intensity values of 3,319 protein spots that were observed in more than 80% of the protein expression profiles of the common internal control sample. Results of hierarchical clustering were associated with histological grouping: the seven normal liver tissues, 11 adjacent nontumor tissues, six well-differentiated HCCs, and one moderately-differentiated HCC were grouped together, while the 13 moderately-differentiated HCCs and seven poorly-differentiated HCCs were clustered together forming a separate group (Fig. 2A). Principal component analysis also showed similar results; normal and adjacent nontumor tissues were grouped together while well-differentiated tumors were segregated from the group of moderately-differentiated or poorly-differentiated tumors (Fig. 2B). These observations suggested that the overall features of the proteome may reflect the major histological patterns.

To identify the proteins that are differentially expressed in the five tissue groups examined, we performed a Kruskal-Wallis test and applied Bonferroni adjustment. We selected the protein spots such that the Bonferroni adjusted P value was <0.01 and the expression ratio between groups with the greatest difference was at least three times or more. Consequently, we found 41 protein spots meeting this criterion (Supporting Fig. 1). The expression pattern of these selected 41 protein spots in all tissue samples is shown in Fig. 2C. Using hierarchical clustering, we found that the protein spots were subdivided into clusters A and B, based on whether their intensity was upregulated or downregulated in the group of moderately-differentiated HCCs and poorly-differentiated HCCs (Fig. 2C).

Protein Identification and Network Analysis. Mass spectrometric study resulted in the identification of 26 unique proteins corresponding to the 41 protein spots (Fig. 2C, right side; Table 1; Supporting Table 2). Functional classification according to Gene Ontology (www.geneontology.org) demonstrated that a large proportion of the identified proteins are involved in amino acid metabolism, oxidoreduction, and lipid metabolism (Fig. 3A; Table 1). The proteins corresponding to the protein spots in clusters A and B were classified according to their known function (Fig. 3B,C; Table 1). Proteins in clusters

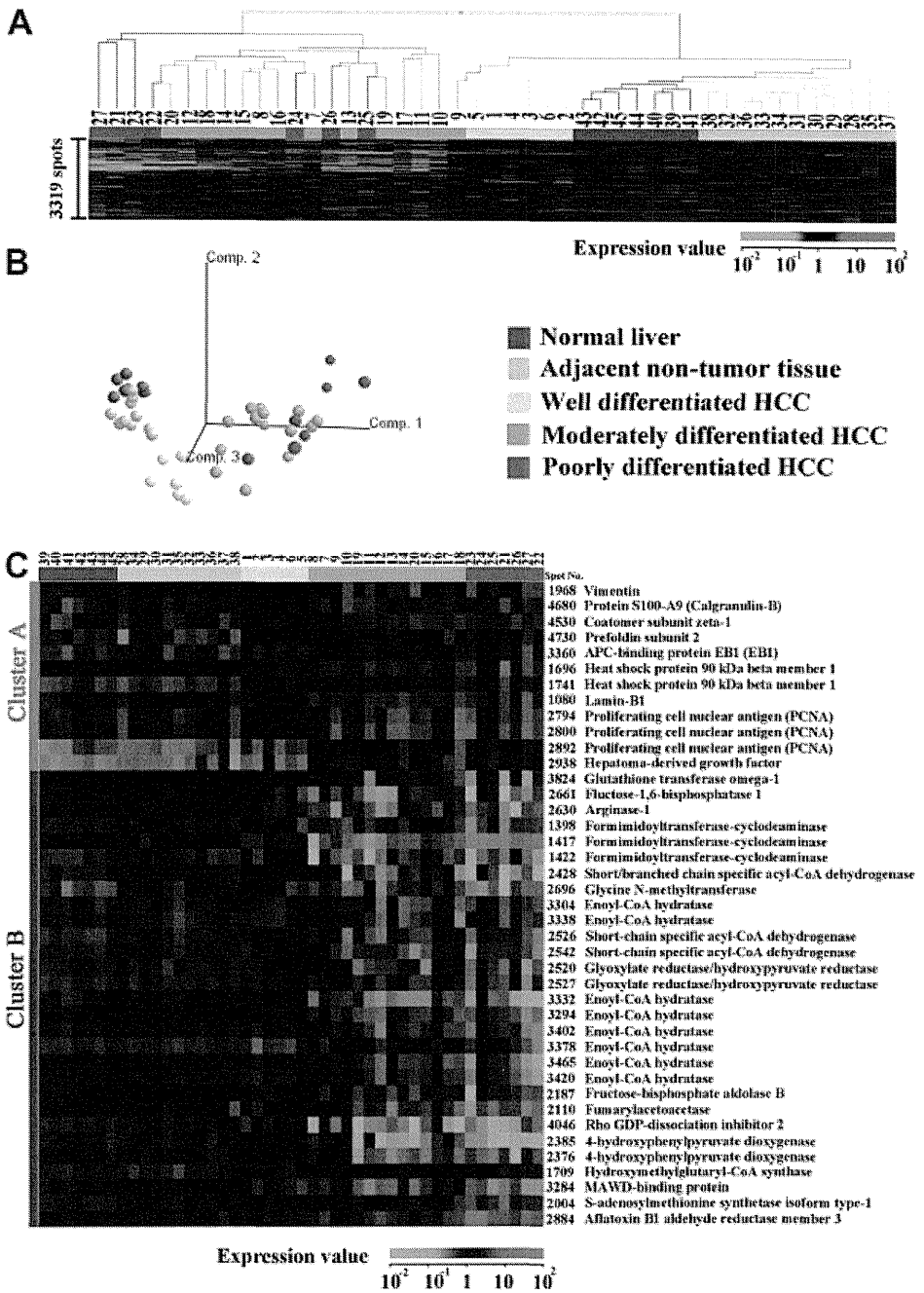

Fig. 2. Proteomic classification of tissue samples and identification of proteins with different expression levels between the sample groups. (A) Hierarchical clustering and (B) principal component analysis grouped the tissue samples based on the intensity of 3319 protein spots. (C) Heat map of the 41 selected protein spots is shown. The results of protein identification are demonstrated in the right side of (C).

A included ones involved in cell proliferation, protein folding, and cytoskeletal/structural proteins. Proteins in cluster B included ones involved in amino acid metabolism, oxidoreduction, and lipid metabolism, all of which maintain normal hepatic functions. Western blotting results were consistent with the 2D-DIGE results, validating the differential expression of the identified proteins (Supporting Fig. 2A,B).

We explored the biological significance of the altered protein expression patterns by classifying the associated proteins within the context of functional pathways and networks using MetaCore, and we found that 14 of the 26 identified proteins could be functionally linked (Supporting Fig. 3). The transcription factors in this network included c-Myc, hepatocyte nuclear factor 4 alpha, AP-1, HIF1A, and C/EBP beta, which connected five, five,

Table 2. Correlations Between Clinicopathological Features and EB1 Expression

Variable	EB1 Positive (Number of Cases)	EB1 Negative (Number of Cases)	Correlation (EB1) *P* Value*
Age†	61 (48-80)	65 (26-83)	0.161
Gender			0.825
Female	8	25	
Male	32	80	
Virus infection status			0.302
HBV	15	31	
HCV	17	60	
Both	5	6	
None	3	8	
Child-Pugh Classification			1.000
A	37	97	
B	3	8	
Liver cirrhosis			0.502
Absence	32	77	
Presence	8	28	
AFP (ng/mL)†			**<0.001**
	343.5 (3-27170)	20.3 (1-9994)	
TNM Stage			**<0.001**
I or II	20	89	
III or IV	20	16	
Tumor number			1.000
Single	31	81	
Multiple	9	24	
Tumor size (mm)†			**0.008**
	45 (13-155)	30 (6-185)	
Differentiation			**<0.001**
Well differentiated	0	24	
Moderately differentiated	9	73	
Poorly differentiated	31	8	
Portal vein invasion			**<0.001**
Absence	8	79	
Presence	32	26	
Intrahepatic metastasis			**<0.001**
Absence	22	90	
Presence	18	15	

Bold indicates significant values. HBV, hepatitis B virus; HCV, hepatitis C virus; AFP, alpha-fetoprotein
*Fisher exact test for categorical variables and Mann-Whitney *U* test for continuous variables.
†Expressed as median (range).

three, two, and one genes, respectively. Other proteins responsible for the regulation of multiple proteins included Ras superfamily proteins such as RhoA, CDC42, and Rac1.

Clinical Significances of EB1 Expression in HCC. Among the identified proteins, EB1 is controlled by c-Myc, RhoA and CDC42, which have all been linked to HCC malignancy in previous reports[18-21] (Fig. 3D). For this reason, we further examined the relationship of EB1 with certain clinicopathological parameters in an additional 145 HCC cases that were not included in the proteomic study, employing immunohistochemistry. Immunohistochemical staining for EB1 was observed in the cytoplasm of tumor cells, inflammatory cells, and bile duct epithelium, while hepatocytes in nontumor areas showed no immunostaining (Fig. 4). The EB1-positive and EB1-negative tumor tissues had significantly different histological differentiation, alpha-fetoprotein expression, TNM stage, tumor size, portal vein invasion status, and intrahepatic metastasis status ($P < 0.01$; Table 2). As these parameters have been correlated with the clinical outcome of patients with HCC, we further investigated the correlation of EB1 with prognostic data. As shown in the Kaplan-Meier survival curve (Fig. 5), patients with EB1-positive HCC tumors had significantly worse prognosis than those with EB1-negative HCC tumors, in terms of both overall survival rate ($P < 0.0001$) and cumulative recurrence rate ($P < 0.0001$). Univariate and multivariate analyses revealed that EB1 is an independent prognostic factor for overall survival (hazard ratio, 2.256; 95% confidence interval, 1.337-3.807; $P = 0.002$) and recurrence (hazard ratio, 2.740; 95% confidence interval, 1.771-4.239; $P < 0.001$) along with other established clinicopathological parameters such as liver cirrhosis, por-

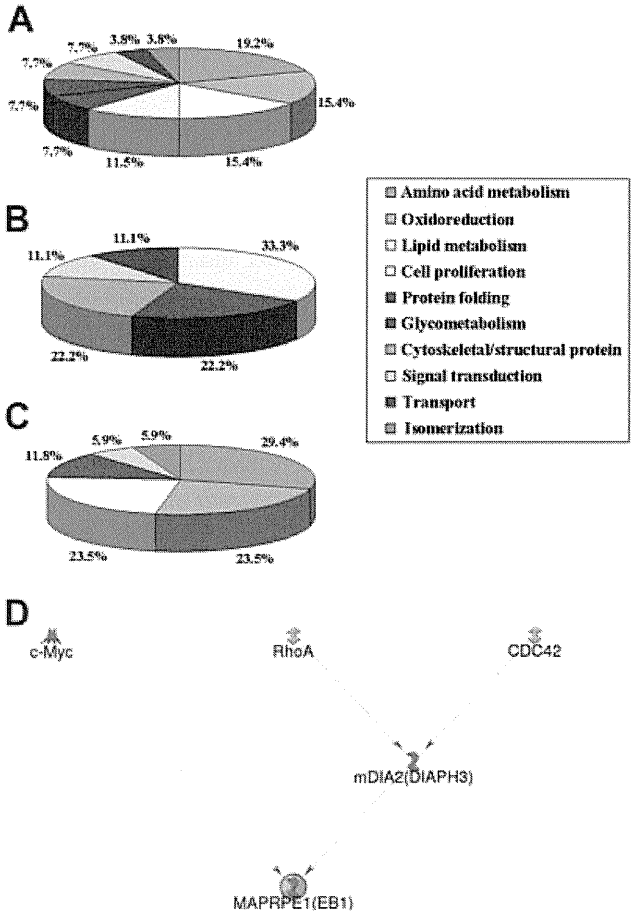

Fig. 3. Functional classification and network analysis of the identified proteins. (A) Functional classification of all proteins, (B) proteins in cluster (A), and (C) proteins in cluster (B). Clusters (A) and (B) are shown in Fig. 2. (D) EB1 is controlled by c-Myc, RhoA, and CDC42, which have all been linked to HCC malignancy. The differently colored nodes represent transcription factors (red shape), Ras-superfamilies (light blue shapes), and other proteins (blue shapes). The green line indicates a positive effect and the gray indicates an unspecified effect.

tal vein invasion, tumor number, and intrahepatic metastasis (Table 3).

Discussion

The need for improvement of the management of HCC has led to a strong demand for the development of novel prognostic biomarkers for HCC. Global genomic and transcriptomic expression studies have been conducted to detect such prognostic molecular biomarkers for HCC. For example, using array-based comparative genomic hybridization analysis, chromosomal loss on 17p13.3 and gain on 8q11 were shown to have significant effects on patient outcome.[22] Using complementary DNA microarray technology, osteopontin was identified as a critical player in HCC metastasis,[23] and AP-1 transcription factors were shown to have key roles in the development of a poor-prognosis subtype of HCC.[24] In contrast, few such studies have been performed using a proteomic approach.[11] Here we present the results of such a proteomic study, and propose EB1 as a prognostic biomarker for HCC.

In this study, we examined HCC tissues classified according to their histological differentiation. As the degree of histological differentiation is a hallmark of the malignant potential of HCC, the proteomic background of HCC differentiation may involve key proteins for HCC progression. Unsupervised classification of tissues based on their protein expression profiles without any *a priori* assumptions was associated with their histological presentation, indicating that the overall features of the proteome may reflect the major histological differences between tissues. We subsequently identified 26 proteins that showed the most variable expression between the groups with different histology.

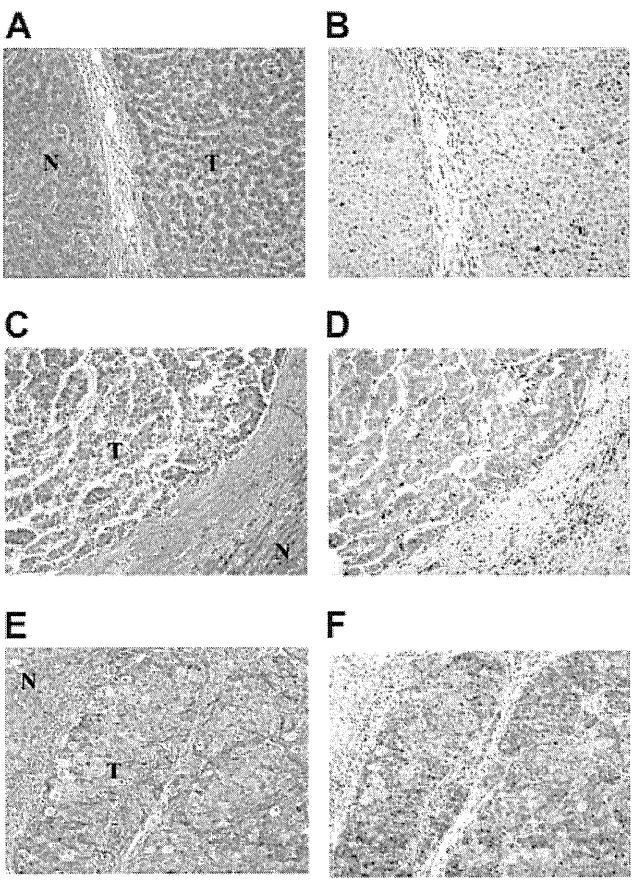

Fig. 4. Expression of EB1 in HCC tissues with different histological differentiation. (A,B) Well-differentiated, (C,D) moderately-differentiated, (E,F) and poorly-differentiated HCCs were examined. (A,C,E) Hematoxylin and eosin-stained tissues; (B,D,F) tissues stained with anti-EB1 antibody. Note that EB1 expression correlated with the degree of histological differentiation. Nontumor liver and HCC are indicated by (N) and (T), respectively.

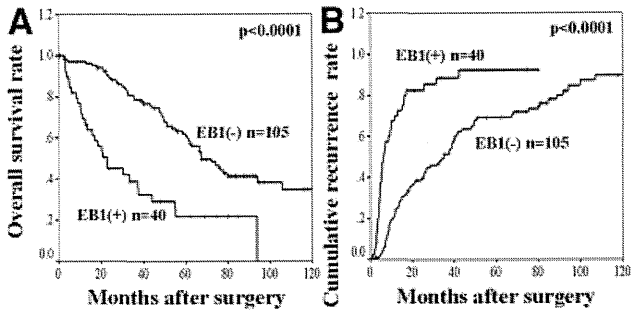

Fig. 5. Correlation of EB1 expression with clinical outcome of HCC patients after curative resection. The patients with HCC tissues showing EB1 expression had poorer prognosis in terms of (A) overall survival and (B) overall recurrence.

Functional classification demonstrated that proteins associated with cell proliferation, protein folding, and cytoskeletal structure were increased, and proteins associated with amino acid metabolism, oxidoreduction, and lipid metabolism were reduced during HCC progression. These findings suggest that the proteins with increased expression during pathological progression have a different functional tendency compared to those with reduced expression. The different proteomic aberrations observed in the varying stages of cancer progression, as reflected in the different histology groups, are unlikely to represent random events. In contrast to the functional classification of the proteins, the chromosomal localization of the genes corresponding to the identified proteins, as identified by searching the National Center for Biotechnology Information database (Table 1), did not have an obvious tendency. These observations suggest that proteomic studies may provide unique information not generated by genomic studies.

Network analysis using literature mining revealed that the identified proteins were functionally linked to certain transcription factors and Ras superfamilies. The transcription factors that linked the identified proteins are known to be frequently activated in HCCs. For instance, c-Myc amplification has been frequently observed in HCCs and is associated with poor prognosis.[18,19] Liu et al.[25] have reported that AP-1 is frequently activated at the early stages of HCC. HIF1A is also important in the progression of hepatocarcinogenesis.[26] Other proteins responsible for the regulation of multiple proteins have also been reported to be correlated with HCC malignancy. Overexpression of RhoA[20] is associated with poor prognosis in HCC, and Rac activation is associated with metastasis of HCC.[27] Activation of CDC42 was involved in the metastasis of HCC cells.[21] The proteins we identified may be downstream effectors of known key regulators of carcinogenesis and tumor progression. Although correlations between these molecules and HCC progression have been independently and separately reported, the present global protein expression study enabled a panoramic view of the molecular background of the progression of HCC.

Our study showed the prognostic value of EB1 expression in HCC. EB1 has been identified as a protein bound to the APC tumor suppressor gene product.[28] In vitro wounding assays revealed that EB1 and APC promote cell migration, stabilizing microtubules in a coordinate manner.[29] EB1 inhibits the ability of APC to bind to actin filaments, which may be required for maintenance of cell-cell adhesion.[30] Recently, Wang et al.[31] reported that in esophageal cancer, overexpression of EB1 promotes cell growth by activating the beta-catenin/T-cell factor pathway, and this pathway is often activated in HCC.[32] Taken together, the interaction of EB1 and APC may play a key role in cytoskeleton organization, cell migration and proliferation, and its aberrant regulation could affect the malignant behavior of HCC, probably resulting in poor prognosis for HCC patients.

Network analysis has revealed that c-Myc, RhoA, and CDC42 regulate the expression and function of EB1. The expression of EB1 is controlled by c-Myc[33] and c-Myc amplification has prognostic significance in HCC.[18] EB1 functions downstream of RhoA and CDC42 by interacting with mDia2,[29,34,35] and both RhoA and CDC42 have also been linked to HCC malignancy.[20,21] Taken together, we considered that EB1 may also be associated with poor prognosis.

Our findings can be of use in the search for biomarker identification and development. We studied the relationship of EB1 expression with clinical outcome of the HCC patients in additional 145 cases. Univariate and multivariate analyses revealed that EB1 is an independent prognostic factor for both recurrence and survival of HCC patients. Our results indicate that EB1 expression may be used as a novel prognostic biomarker of HCC. The correlation between EB1 expression and prognosis in HCC has not been examined or demonstrated previously.

The expression of EB1 was observed only in moderately or poorly differentiated HCC in this study (Table 2), and the prognostic utility of EB1 expression is therefore limited to patients with these tumors. The overall survival rate of patients with well-differentiated HCC was significantly higher than that of patients with poorly-differentiated or moderately-differentiated tumors (Table 3), a finding that is consistent with the report by Ariizumi et al.,[36] in which the 5-year survival rate was 78.1%, 49.0%, and 37.4% for the well-differentiated, moderately-differentiated, and poorly-differentiated tumors, respectively. The evaluation of EB1 expression could therefore provide prognostic information for the sub-

Table 3. Univariate and Multivariate Analyses of Prognostic Factors for Patients with HCC

		Univariate Analysis			
		Survival		Recurrence	
Variable	n	5-Years (%)	*P* Value	5-Years (%)	*P* Value
Age*			**0.7909**		0.6517
<64	76	53.8 ± 6.2		77.8 ± 5.2	
≥64	69	48.8 ± 6.3		73.7 ± 5.5	
Gender			0.9721		0.9862
Female	33	51.6 ± 9.2		78.1 ± 7.5	
Male	112	51.3 ± 5.1		75.2 ± 4.4	
Virus infection status			**0.3794**		0.0827
HBV	46	53.1 ± 8.0		60.0 ± 7.8	
HCV	77	54.3 ± 6.1		81.1 ± 4.6	
Both	11	36.4 ± 14.5		87.9 ± 11.0	
None	11	40.0 ± 15.5		81.8 ± 11.6	
Child-Pugh Classification			**0.0407**		0.1315
A	134	52.9 ± 4.6		74.7 ± 4.0	
B	11	34.1 ± 15.0		100.0 ± 0.0	
Liver cirrhosis			**0.0277**		0.6586
Absence	109	57.6 ± 5.1		74.6 ± 4.4	
Presence	36	35.2 ± 8.1		79.0 ± 7.4	
AFP*			**0.0532**		**0.0210**
<27.2	70	60.4 ± 6.2		67.1 ± 6.1	
≥27.2	73	41.4 ± 6.2		85.8 ± 4.3	
TNM Stage			**<0.0001**		**<0.0001**
I or II	109	61.9 ± 5.0		69.6 ± 4.7	
III or IV	36	16.2 ± 7.1		94.3 ± 3.9	
Tumor number			0.0856		**0.0238**
Single	112	55.9 ± 5.0		70.9 ± 4.6	
Multiple	33	36.8 ± 9.0		90.9 ± 5.0	
Tumor size (mm)*			0.0627		**0.0178**
<35	66	62.1 ± 6.3		72.9 ± 5.8	
≥35	79	42.5 ± 6.0		78.2 ± 4.9	
Differentiation			**<0.0001**		**<0.0001**
Well differentiated	24	73.9 ± 9.2		76.3 ± 9.2	
Moderately differentiated	82	59.6 ± 5.8		66.2 ± 5.6	
Poorly differentiated	39	16.3 ± 7.3		95.9 ± 3.8	
Portal vein invasion			**<0.0001**		**0.0001**
Absence	87	67.7 ± 5.3		68.4 ± 5.3	
Presence	58	24.7 ± 6.4		86.6 ± 4.8	
Intrahepatic metastasis			**<0.0001**		**<0.0001**
Absence	112	60.7 ± 4.9		70.6 ± 4.6	
Presence	33	19.0 ± 7.4		93.7 ± 4.3	
EB1 expression			**<0.0001**		**<0.0001**
Negative	105	62.1 ± 5.0		69.3 ± 4.8	
Positive	40	22.0 ± 7.4		92.2 ± 4.7	

	Multivariate Analysis				
	Beta	SE	HR	95% CI	*P* value
Survival					
Liver cirrhosis	0.922	0.258	2.515	1.517-4.170	**<0.001**
Portal vein invasion	0.670	0.301	1.955	1.083-3.528	**0.026**
Intrahepatic metastasis	0.699	0.289	2.012	1.143-3.544	**0.015**
EB1 expression	0.814	0.267	2.256	1.337-3.807	**0.002**
Recurrence					
Tumor number	0.594	0.213	1.811	1.192-2.752	**0.005**
Intrahepatic metastasis	1.030	0.227	2.802	1.795-4.375	**<0.001**
EB1 expression	1.008	0.223	2.740	1.771-4.239	**<0.001**

Bold indicates significant values. *Two groups were divided by the median. HBV, hepatitis B virus; HCV, hepatitis C virus; AFP, alpha-fetoprotein; Beta, regression coefficient; SE, standard error; HR, hazard ratio; CI, confidence interval.

groups of HCC, which could benefit from a more refined prognostic protocol.

Our list of identified proteins also included gene products reported as prognostic biomarker candidates (Fig. 2C). Expression of both hepatoma-derived growth factor[37] and proliferating cell nuclear antigen[38] have been correlated with poor differentiation, shorter survival periods, and higher incidence of recurrence in HCC patients. Overexpression of vimentin has been associated with the metastasis in HCC.[39] The relation between HCC differentiation and poor prognosis may be explained by these proteins and EB1, and the combined use of these biomarker candidates may improve the diagnosis and prognostic performance.

In conclusion, through the present global protein expression study the molecular background of histological differentiation in HCC was revealed and EB1 was established as a prognostic biomarker for both recurrence and survival. Poor outcomes in HCC are mainly due to postsurgical tumor recurrence, but recent advances in adjuvant therapies have improved survival periods for patients with recurrence.[40] The immunohistochemical examination of EB1 expression will help identify patients with high risk for recurrence, and close postoperative follow-up and additional treatment may improve the clinical outcome of these patients. Taken together, our results provide the possibility of novel strategies for HCC management.

Acknowledgment: The excellent technical support of Yukiko Fujie and Mina Fujishiro with the electrophoresis is greatly appreciated.

References

1. Bosch FX, Ribes J, Borras J. Epidemiology of primary liver cancer. Semin Liver Dis 1999;19:271-285.
2. Pisani P, Parkin DM, Bray F, Ferlay J. Estimates of the worldwide mortality from 25 cancers in 1990. Int J Cancer 1999;83:18-29.
3. Parkin DM, Pisani P, Ferlay J. Estimates of the worldwide incidence of 25 major cancers in 1990. Int J Cancer 1999;80:827-841.
4. El-Serag HB, Mason AC. Rising incidence of hepatocellular carcinoma in the United States. N Engl J Med 1999;340:745-750.
5. Taylor-Robinson SD, Foster GR, Arora S, Hargreaves S, Thomas HC. Increase in primary liver cancer in the UK, 1979-94. Lancet 1997;350: 1142-1143.
6. Ker CG, Chen HY, Chen KS, Jeng IJ, Yang MY, Juan CC, et al. Clinical significance of cell differentiation in hepatocellular carcinoma. Hepatogastroenterology 2003;50:475-479.
7. Hu Z, Evarts RP, Fujio K, Marsden ER, Thorgeirsson SS. Expression of hepatocyte growth factor and c-met genes during hepatic differentiation and liver development in the rat. Am J Pathol 1993;142:1823-1830.
8. Suzuki T, Yano H, Nakashima Y, Nakashima O, Kojiro M. Beta-catenin expression in hepatocellular carcinoma: a possible participation of beta-catenin in the dedifferentiation process. J Gastroenterol Hepatol 2002;17: 994-1000.
9. Diamond DL, Proll SC, Jacobs JM, Chan EY, Camp DG 2nd, Smith RD, et al. HepatoProteomics: applying proteomic technologies to the study of liver function and disease. HEPATOLOGY 2006;44:299-308.
10. Yokoo H, Kondo T, Okano T, Nakanishi K, Sakamoto M, Kosuge T, et al. Protein expression associated with early intrahepatic recurrence of hepatocellular carcinoma after curative surgery. Cancer Sci 2007;98: 665-673.
11. Yi X, Luk JM, Lee NP, Peng J, Leng X, Guan XY, et al. Association of mortalin (HSPA9) with liver cancer metastasis and prediction for early tumor recurrence. Mol Cell Proteomics 2008;7:315-325.
12. Hatakeyama H, Kondo T, Fujii K, Nakanishi Y, Kato H, Fukuda S, et al. Protein clusters associated with carcinogenesis, histological differentiation and nodal metastasis in esophageal cancer. Proteomics 2006; 6:6300-6316.
13. Hirohashi S, Isak KG, Kojiro M, Wanless IR, Theise ND, Tsukuma H, et al. Hepatocellular carcinoma. Lyon, France: IARC Press; 2000:159-172.
14. Greene FL, Page DL, Fleming ID, Fritz A, Balch CM, Haller DG, et al. AJCC Cancer Staging Manual. 6th ed. Chicago: Springer; 2002:131-144.
15. Kondo T, Seike M, Mori Y, Fujii K, Yamada T, Hirohashi S. Application of sensitive fluorescent dyes in linkage of laser microdissection and two-dimensional gel electrophoresis as a cancer proteomic study tool. Proteomics 2003;3:1758-1766.
16. Kondo T, Hirohashi S. Application of highly sensitive fluorescent dyes (CyDye DIGE Fluor saturation dyes) to laser microdissection and two-dimensional difference gel electrophoresis (2D-DIGE) for cancer proteomics. Nat Protoc 2006;1:2940-2956.
17. Kaplan E, Meier P. Nonparametric estimation from incomplete observations. J Am Stat Assoc 1958;53:457-481.
18. Wang Y, Wu MC, Sham JS, Zhang W, Wu WQ, Guan XY. Prognostic significance of c-Myc and AIB1 amplification in hepatocellular carcinoma. A broad survey using high-throughput tissue microarray. Cancer 2002;95: 2346-2352.
19. Abou-Elella A, Gramlich T, Fritsch C, Gansler T. c-Myc amplification in hepatocellular carcinoma predicts unfavorable prognosis. Mod Pathol 1996:9:95-98.
20. Li XR, Ji F, Ouyang J, Wu W, Qian LY, Yang KY. Overexpression of RhoA is associated with poor prognosis in hepatocellular carcinoma. Eur J Surg Oncol 2006;32:1130-1134.
21. Xie L, Qin W, Li J, He X, Zhang H, Yao G, et al. BNIPL-2 promotes the invasion and metastasis of human hepatocellular carcinoma cells. Oncol Rep 2007;17:605-610.
22. Katoh H, Shibata T, Kokubu A, Ojima H, Loukopoulos P, Kanai Y, et al. Genetic profile of hepatocellular carcinoma revealed by array-based comparative genomic hybridization: identification of genetic indicators to predict patient outcome. J Hepatol 2005;43:863-874.
23. Ye QH, Qin LX, Forgues M, He P, Kim JW, Peng AC, et al. Predicting hepatitis B virus-positive metastatic hepatocellular carcinomas using gene expression profiling and supervised machine learning. Nat Med 2003;9: 416-423.
24. Lee JS, Heo J, Libbrecht L, Chu IS, Kaposi-Novak P, Calvisi DF, et al. A novel prognostic subtype of human hepatocellular carcinoma derived from hepatic progenitor cells. Nat Med 2006;12:410-416.
25. Liu P, Kimmoun E, Legrand A, Sauvanet A, Degott C, Lardeux B, et al. Activation of NF-kappa B, AP-1 and STAT transcription factors is a frequent and early event in human hepatocellular carcinoma. J Hepatol 2002;37:63-71.
26. Tanaka H, Yamamoto M, Hashimoto N, Miyakoshi M, Tamakawa S, Yoshie M, et al. Hypoxia-independent overexpression of hypoxia-inducible factor 1alpha as an early change in mouse hepatocarcinogenesis. Cancer Res 2006;66:11263-11270.
27. Lee TK, Poon RT, Yuen AP, Man K, Yang ZF, Guan XY, et al. Rac activation is associated with hepatocellular carcinoma metastasis by up-regulation of vascular endothelial growth factor expression. Clin Cancer Res 2006;12:5082-5089.
28. Su LK, Burrell M, Hill DE, Gyuris J, Brent R, Wiltshire R, et al. APC binds to the novel protein EB1. Cancer Res 1995;55:2972-2977.
29. Wen Y, Eng CH, Schmoranzer J, Cabrera-Poch N, Morris EJ, Chen M, et al. EB1 and APC bind to mDia to stabilize microtubules downstream of Rho and promote cell migration. Nat Cell Biol 2004;6:820-830.

30. Moseley JB, Bartolini F, Okada K, Wen Y, Gundersen GG, Goode BL. Regulated binding of adenomatous polyposis coli protein to actin. J Biol Chem 2007;282:12661-12668.
31. Wang Y, Zhou X, Zhu H, Liu S, Zhou C, Zhang G, et al. Overexpression of EB1 in human esophageal squamous cell carcinoma (ESCC) may promote cellular growth by activating beta-catenin/TCF pathway. Oncogene 2005;24:6637-6645.
32. Thompson MD, Monga SP. WNT/beta-catenin signaling in liver health and disease. HEPATOLOGY 2007;45:1298-1305.
33. Chen Y, Blackwell TW, Chen J, Gao J, Lee AW, States DJ. Integration of genome and chromatin structure with gene expression profiles to predict c-MYC recognition site binding and function. PLoS Comput Biol 2007;3:e63.
34. Alberts AS, Bouquin N, Johnston LH, Treisman R. Analysis of RhoA-binding proteins reveals an interaction domain conserved in heterotrimeric G protein beta subunits and the yeast response regulator protein Skn7. J Biol Chem 1998;273:8616-8622.
35. Peng J, Wallar BJ, Flanders A, Swiatek PJ, Alberts AS. Disruption of the Diaphanous-related formin Drf1 gene encoding mDia1 reveals a role for Drf3 as an effector for Cdc42. Curr Biol 2003;13:534-545.
36. Ariizumi S, Takasaki K, Yamamoto M, Ohtsubo T, Katsuragawa H, Katagiri S. Histopathologic differentiation of the main nodule determines outcome after hepatic resection for synchronous multicentric hepatocellular carcinomas. Hepatogastroenterology 2004;51:500-504.
37. Hu TH, Huang CC, Liu LF, Lin PR, Liu SY, Chang HW, et al. Expression of hepatoma-derived growth factor in hepatocellular carcinoma. Cancer 2003;98:1444-1456.
38. Kitamoto M, Nakanishi T, Kira S, Kawaguchi M, Nakashio R, Suemori S, et al. The assessment of proliferating cell nuclear antigen immunohistochemical staining in small hepatocellular carcinoma and its relationship to histologic characteristics and prognosis. Cancer 1993;72:1859-1865.
39. Hu L, Lau SH, Tzang CH, Wen JM, Wang W, Xie D, et al. Association of vimentin overexpression and hepatocellular carcinoma metastasis. Oncogene 2004;23:298-302.
40. Shah SA, Cleary SP, Wei AC, Yang I, Taylor BR, Hemming AW, et al. Recurrence after liver resection for hepatocellular carcinoma: risk factors, treatment, and outcomes. Surgery 2007;141:330-339.

Published OnlineFirst April 18, 2012; DOI:10.1158/1078-0432.CCR-12-0183

Clinical Cancer Research

Decreased Selenium-Binding Protein 1 Enhances Glutathione Peroxidase 1 Activity and Downregulates HIF-1 α to Promote Hepatocellular Carcinoma Invasiveness

Cheng Huang, Guangyu Ding, Chengyu Gu, et al.

Clin Cancer Res 2012;18:3042-3053. Published OnlineFirst April 18, 2012.

Published OnlineFirst April 18, 2012; DOI:10.1158/1078-0432.CCR-12-0183

Human Cancer Biology

Clinical Cancer Research

Decreased Selenium-Binding Protein 1 Enhances Glutathione Peroxidase 1 Activity and Downregulates HIF-1α to Promote Hepatocellular Carcinoma Invasiveness

Cheng Huang[1], Guangyu Ding[1], Chengyu Gu[1], Jian Zhou[1], Ming Kuang[3], Yuan Ji[2], Yifeng He[1], Tadashi Kondo[4], and Jia Fan[1]

Abstract

Purpose: We aimed to characterize the role of selenium-binding protein 1 (SBP1) in hepatocellular carcinoma (HCC) invasiveness and underlying clinical significance.

Experimental Design: SBP1 expression was measured in stepwise metastatic HCC cell lines by Western blotting. The role of SBP1 in HCC was investigated using siRNA. Immunofluorescence analyses were used to detect the interaction between SBP1 and glutathione peroxidase 1 (GPX1). Nineteen fresh tumor tissues and 323 paraffin-embedded samples were used to validate *in vitro* findings and to detect the prognostic significance of SBP1, respectively.

Results: Inhibition of SBP1 effectively increased cell motility, promoted cell proliferation, and inhibited apoptosis only under oxidative stress; it also greatly enhanced GPX1 activity without altering GPX1 expression and downregulated hypoxia-inducible factor-1α (HIF-1α) expression. SBP1 and GPX1 formed nuclear bodies and colocalized under oxidative stress. In freshly isolated clinical HCC tissues, decreased SBP1 was linked with increased GPX1 activity and correlated with vascular invasion. Tumor tissue microarrays indicated that SBP1 was an independent risk factor for overall survival and disease recurrence; patients with lower SBP1 expression experienced shorter overall survival periods and higher rates of disease recurrence ($P < 0.001$). Further analyses indicated that the predictive power of SBP1 was more significant for patients beyond the Milan criteria than patients within the Milan criteria.

Conclusions: Decreased expression of SBP1 could promote tumor invasiveness by increasing GPX1 activity and diminishing HIF-1α expression in HCC; SBP1 could be a novel biomarker for predicting prognosis and guiding personalized therapeutic strategies, especially in patients with advanced HCC. *Clin Cancer Res; 18(11); 3042–53. ©2012 AACR.*

Introduction

Selenium is an essential trace element with cancer-preventing activities that have been shown in many epidemiologic studies (1–3). The cellular biochemistry of selenium is a complex system that involves the expression of a wide range of selenium-containing proteins (4–6). Of these proteins, a 56-kDa molecule termed selenium-binding protein 1 (SBP1) was found to be the possible mediator of selenium's anticancer functions (7, 8). SBP1 is expressed in various cell types, including liver, heart, and kidney (2), and previous studies have established a solid connection between SBP1 and cancer. Decreased SBP1 was found in a vast number of human cancers, such as colorectal cancer (9), lung adenocarcinomas (10), ovarian cancer (11), gastric cancer (12), and hepatocellular carcinoma (HCC; ref. 13). However, the molecular mechanism underlying the tumor suppressive functions of SBP1 remains unclear.

Glutathione peroxidase 1 (GPX1) is also an important selenium-containing protein, in which selenium is a constituent of the amino acid selenocysteine. GPX1 is a ubiquitously expressed antioxidant enzyme that scavenges organic hydroperoxides and protects cells from reactive oxygen species (ROS) and hydrogen peroxide–induced or -dependent apoptotic injury (14, 15). Elevated GPX1 activity was reported to protect cancer cells from oxidative stress and anticancer agents (16–18). Previous studies using

Authors' Affiliations: [1]Liver Cancer Institute, [2]Department of Pathology, Zhongshan Hospital and Shanghai Medical School, Fudan University, Key Laboratory for Carcinogenesis & Cancer Invasion, the Chinese Ministry of Education, Shanghai; [3]Department of Hepatobiliary Surgery, The First Affiliated Hospital of Sun Yat-sen University, Guangzhou, PR China; and [4]Division of Pharmacoproteomics, National Cancer Center Research Institute, Tokyo, Japan

Note: Supplementary data for this article are available at Clinical Cancer Research Online (http://clincancerres.aacrjournals.org/).

C. Huang, G. Ding, and C. Gu contributed equally to this work.

Corresponding Authors: Jia Fan, Liver Cancer Institute, Fudan University, 136 Yi Xue Yuan Rd, Shanghai 200032, PR China. Phone: 0086-21-64037181; Fax: 0086-21-64037181; E-mail: fan.jia@zs-hospital.sh.cn and Tadashi Kondo, Division of Pharmacoproteomics, National Cancer Center Research Institute, 5-1-1 Tsukiji, Chuo-ku, Tokyo 104-0045, Japan. E-mail: proteomebioinformatics@gmail.com

doi: 10.1158/1078-0432.CCR-12-0183

Published OnlineFirst April 18, 2012; DOI:10.1158/1078-0432.CCR-12-0183

Translational Relevance

Selenium-binding protein 1 (SBP1) has been considered to be a protective agent against cancer. However, little is known about the function of SBP1 or its potential applications as a prognostic marker in hepatocellular carcinoma (HCC). Our findings indicate that SBP1 may act as a pro-oxidant rather than antioxidant through the interaction with glutathione peroxidase 1 and hypoxia-inducible factor-1α. Thus, the use of antioxidants such as glutathione in patients with HCC, especially patients with advanced-stage cancer, should be completed with caution. Furthermore, determination of SBP1 expression is especially useful for personalized therapeutic strategies and decisions about individuals beyond Milan criteria who could benefit from more aggressive treatment, such as chemotherapy or liver transplantation.

coimmunoprecipitation showed that these 2 distinct selenium-containing proteins (GPX1 and SBP1) can form a physical association that facilitates their interactions (19), but their possible roles in cancer development are still unknown. SBP1 is also known to have a hypoxia response element in its promoter region and to be a target gene of hypoxia-inducible factor-1α (HIF-1α; ref. 20), which is a fundamental mediator of cellular adaptation to microenvironmental stress, especially oxidative stress (21). The relationship between GPX1 and oxidative stress and the multifunctional role of HIF-1α in cancer biology may be associated with the antitumor activity of SBP1.

HCC is the sixth most common malignancy and the third leading cause of cancer death worldwide (22). Although early diagnosis and surgical treatments have significantly improved overall patient outcomes, long-term survival is still low due to high rates of recurrence and metastasis. Resistance toward cytotoxic chemotherapy also affects survival and prognosis in patients with HCC (23). We and other groups have found that the expression of SBP1 is decreased in most HCCs and is associated with poor outcomes (13), but the possible molecular mechanism of SBP1 in HCC biology, particularly in cancer invasion and metastasis, has not been studied. Given the relationship among SBP1, GPX1, HIF-1α, and oxidative stress in the HCC microenvironment, in this study, we aimed to explore the role of SBP1 in cancer invasion and metastasis. We found that decreased SBP1 could promote HCC invasion/metastasis and lead to poor prognosis through the enhancement of GPX1 activity and the downregulation of HIF-1α.

Materials and Methods

Cell lines

The normal liver cell line L-02 and the HCC cell lines HepG2, Hep3B, SMMC7721, Huh 7, and PLC/PRF/5 were purchased from the Institute of Biochemistry and Cell Biology, Chinese Academy of Sciences (CAS). HCC cell lines with stepwise metastatic potential (MHCC97L, MHCC97H, HCCLM3, and HCCLM6, which are HBV-positive cell lines with the same genetic background but different lung metastatic potentials) were established at our institute (24, 25). Cell lines were grown in Dulbecco's Modified Eagle's Medium (DMEM) or RPMI-1640 (Invitrogen/GIBCO) supplemented with 10% FBS (Invitrogen/GIBCO) at 37°C in 5% carbon dioxide.

We used hydrogen peroxide (Sigma) as ROS resources to simulate oxidative stress *in vitro*. A concentration of 300, 100, and 50 μmol/L was used in the apoptosis assay, proliferative assay, and immunofluorescence assay, respectively.

Patients and samples

Patients with HCC ($n = 342$) who underwent surgical treatment at the Zhongshan Hospital at Fudan University (Shanghai, China) were enrolled in this study. Patients were divided into 2 cohorts according to their dates of surgery. To ensure accurate analysis of GPX1 activity, tumor tissue samples were freshly isolated from 19 patients during a 2-week period in 2011 (cohort 1). Tumor specimens used in tissue microarrays (TMA) analyses were consecutively chosen from 323 patients with HCC between 2003 and 2004 (cohort 2). Ethical approval for human subjects was obtained from the Institutional Review Board, and written informed consent was obtained from the patients.

Patients in cohort 1 were classified into 2 groups according to the extent of vascular invasion detected. Patients in cohort 2 were followed up every 2 months during the first postoperative year and at least every 3 to 4 months thereafter until March 15, 2009, 9 of the 323 patients were lost. The median follow-up period was 60 months (range, 2–85 months). Overall survival (OS) was defined as the interval between surgery and death or between surgery and the last observation point. Time to recurrence was defined as the interval between the date of surgery and the date of diagnosis of intrahepatic recurrence and metastasis. Using 24 months as the cutoff value, all cases of recurrence were divided into early recurrence ($n = 147$) or late recurrence ($n = 55$; ref. 26). Preparations of tissue samples are described in the Supplementary Appendix.

Molecular and cell biology assays

Western blotting, quantitative real-time PCR (qRT-PCR), migration analysis, proliferation analysis, apoptosis assay, and immunofluorescence assay were conducted as described previously (27). Detailed information is provided in the Supplementary Appendix.

RNA interference

For siRNA-mediated SBP1 silencing, the following target siRNA sequences were used: sense, CUUGGAGGCACCAAGAAAUTT and antisense, AUUUCUUGGUGCCUCCAAGTT. The RNA duplexes were synthesized by the Genepharma Company. Transfection of the siRNAs into the SMMC7721 cell line was carried out with Lipofectamine 2000 (Invitrogen) according to the manufacturer's instructions.

Published OnlineFirst April 18, 2012; DOI:10.1158/1078-0432.CCR-12-0183

Measurement of GPX1 activity

Measurement of GPX1 activity was conducted as described previously (28). Detailed information is provided in the Supplementary Appendix.

TMAs and immunohistochemistry

TMAs were constructed by the Shanghai Biochip Co., Ltd. The primary antibody used in immunohistochemistry was SBP1 (1:500; MBL). Immunohistochemistry was carried out using a 2-step protocol (Novolink Polymer Detection System; Novocastra). Negative control slides in which the primary antibodies were omitted were included in all assays.

To validate concordance between TMAs and whole tumor sections, we further detected the expression of SBP1 by immunohistochemistry in 50 corresponding whole tumor sections randomly chosen from the 323 cases.

Evaluation of immunohistochemical variables

Immunohistochemical scores were assessed by 2 independent pathologists without knowledge of patient characteristics, and the scores for all cases were compared with check for discrepancies. The final scores were assigned by discussion. Scores were assigned as intensity and percentage of positively staining tumor cell cytoplasm and nuclei in the whole tissue sample. Specifically, the immunostains were scored using a 4-point scale (0–+++) system based on the number of positive cells and the intensity of staining.

Correlations of SBP1 expression profiles with clinical demographics, OS, and recurrence rates were evaluated. Further details about these methods are described in the Supplementary Appendix.

Statistical analysis

The software package SPSS v13.0 (SPSS Inc.) was used for statistical analyses. Univariate and multivariate Cox proportional hazards models were used to identify relevant prognostic factors. Kaplan–Meier survival curves and the log-rank (Mantel–Cox) test were used to compare patient survival and recurrence probability between subgroups (26). All statistical tests were 2-sided, and a P value less than 0.05 was considered statistically significant.

Results

SBP1 is minimally expressed in most human HCC cell lines and inhibits cell migration

We detected the expression levels of SBP1 in current HCC cell lines (Fig. 1A). SBP1 was highly expressed in normal liver cells whereas barely detected in the highly metastatic HCC cell lines (MHCC97L, MHCC97H, HCCLM3, and HCCLM6). HCC cell lines with low metastatic potential also expressed marginal levels of SBP1 with the exception of SMMC7721. SMMC7721 was the only HCC cell line that expressed a high level SBP1, and we chose this cell line for further study. The expression of SBP1 in SMMC7721 72 hours after siRNA transfection was downregulated to a minimal level (Fig. 1B and D) compared with SBP1 expression in the negative control.

Cell migration of SBP1-silenced SMMC7721 cells and negative control cells was assessed via Transwell chambers (Fig. 1C) and wound-healing assays (Fig. 1E). The results showed significant differences indicating that SBP1 greatly inhibits cancer cell migration.

SBP1 inhibits proliferation and induces apoptosis only after hydrogen peroxide treatment

We used the CCK-8 assay to determine whether SBP1 might interfere with cell proliferation and we observed that SBP1 only inhibited cellular proliferation following hydrogen peroxide treatment (Fig. 2A). When cells were cultured in normal medium, SBP1 did not inhibit cell proliferation, and the proliferation rate of the control group was slightly higher than that of the SBP1-silenced group. However, if 100 μmol/L of hydrogen peroxide was added to the culture medium, SBP1 greatly inhibited cell proliferation. The inhibition of proliferation began 24 hours following treatment, and the cell counts of the control group were slightly decreased at 48 and 72 hours whereas the SBP1-silenced group cells were unaffected in the presence of hydrogen peroxide. These results indicated that SBP1 alone could not inhibit cell proliferation.

The apoptosis assay showed results similar to those obtained earlier (Fig. 2B). No significant differences in apoptosis rates were observed between the 2 groups if given normal culture medium. However, if 300 μmol/L of hydrogen peroxide was added and cells were incubated for 24 hours, the apoptosis rate of the SBP1-silenced group was dramatically reduced compared with that of the negative control group, indicating that SBP1 could somehow facilitate the hydrogen peroxide–induced apoptosis.

SBP1 and HIF-1α interactions

Figure 2C showed the interactions of SBP1, HIF-1α, and GPX1 expressions under different conditions. The hydrogen peroxide–treated groups were treated with 50 μmol/L hydrogen peroxide for 24 hours before protein extraction. The expression of HIF-1α was increased by hydrogen peroxide treatment, as shown by the control groups (SMMC7721 and SMMC7721-Mock), and an increase in SBP1 expressions could also be observed in the same groups. This is consistent with the finding that SBP1 is a target gene for HIF-1α (20). However, in the SMMC7721 groups where SBP1 expression was downregulated by siRNA treatment, the expression of HIF-1α was not elevated by hydrogen peroxide treatment. This might indicate that SBP1 could also somehow counter-regulate the expression of HIF-1α following hydrogen peroxide treatment.

The expression of GPX1, however, was not associated with either SBP1 or HIF-1α (Fig. 2C), although a slight increase could be detected following treatment with hydrogen peroxide.

SBP1 greatly inhibits GPX1 activity, not expression level *in vitro*

We measured the activities of GPX1 under different conditions *in vitro* (Fig. 2D). Compared with the control

Published OnlineFirst April 18, 2012; DOI:10.1158/1078-0432.CCR-12-0183

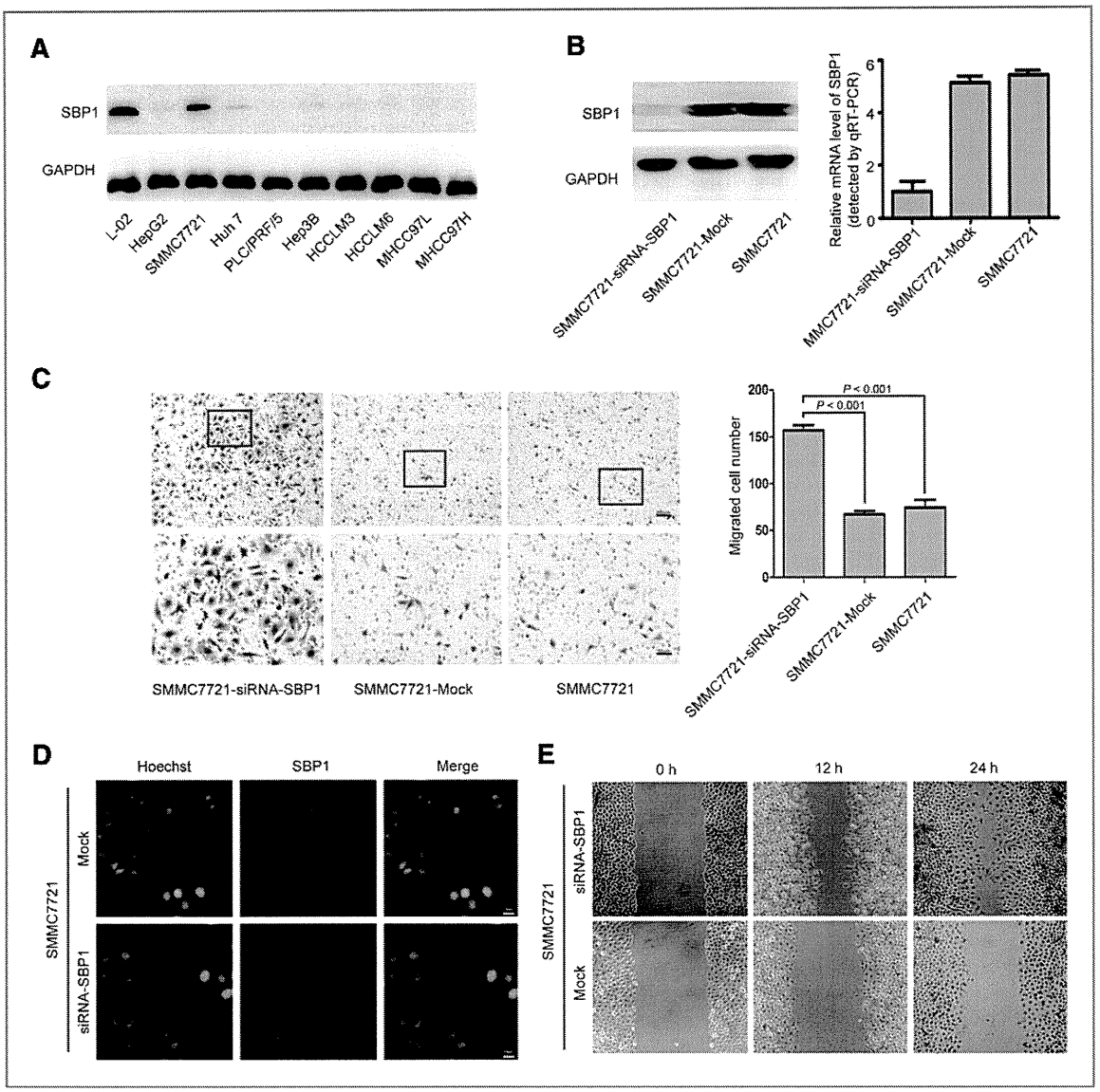

Figure 1. Expression of SBP1 in HCC cell lines and migration analysis of SBP1 by siRNA. A, Western blot analysis of SBP1 expression in cell lines L-02, HepG2, SMMC7721, Huh7, PLC/PRF/5, Hep3B, HCCLM3, HCCLM6, MHCC97L, and MHCC97H. L-02 and SMMC7721 both expressed relatively high levels of SBP1 compared with other HCC cell lines. Glyceraldehyde-3-phosphate dehydrogenase (GAPDH) was used as a loading control. B, both Western blotting and qRT-PCR results showed that SBP1 expression in SMMC7721 cells was downregulated to a marginal level by siRNA treatment. Total protein and RNA were extracted from the cells 72 hours after transfection. C, Transwell assays showed that the number of migrated cells in the SBP1-siRNA group increased significantly compared with those in the control group. Representative data of 3 independent experiments are shown. D, immunofluorescence showed the location of SBP1 in SMMC7721-Mock and SMMC7721-siRNA samples. E, the wounds were nearly closed 24 hours after scratch in the SBP1-siRNA group compared with the control group. All experiments were repeated at least 3 times.

groups, the GPX1 activities in the SBP1-silenced groups had increased by 4- or 5-fold. This dramatic increase in GPX1 activity indicates that SBP1 may greatly inhibit GPX1 activity. Given the fact that the expression levels of GPX1 in different groups were unchanged (Fig. 2C), SBP1 might inhibits GPX1 through a post-translational way.

SBP1 and GPX1 formed special bodies and colocalized in the nuclei following hydrogen peroxide treatment

Under normal conditions, GPX1 localized exclusively in the cytoplasm but SBP1 could be found both in the cytoplasm and the nucleus (Fig. 3A). However, when cells were treated with hydrogen peroxide, we observed that both GPX1 and SBP1 had established specific nuclear bodies,

Published OnlineFirst April 18, 2012; DOI:10.1158/1078-0432.CCR-12-0183

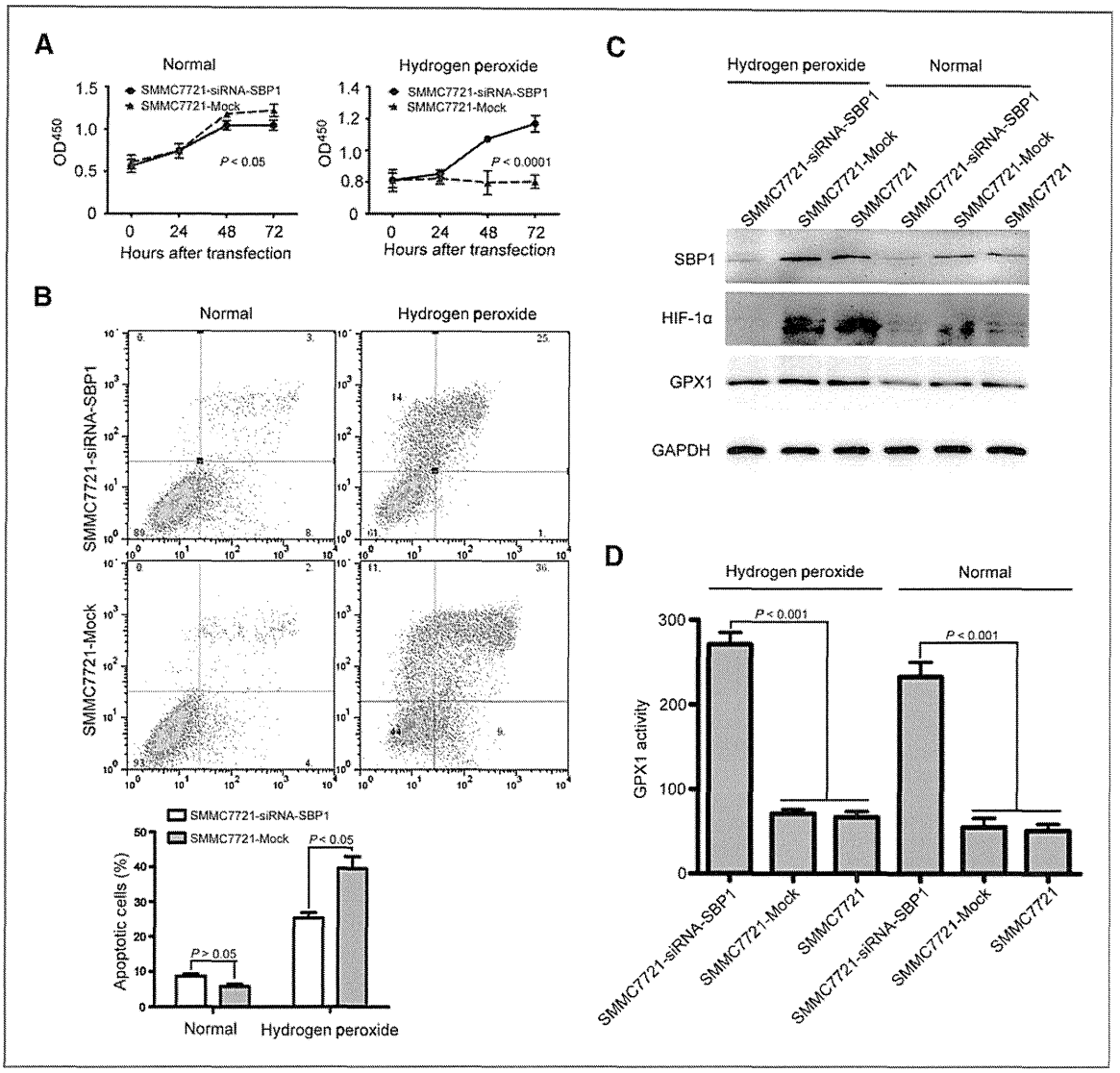

Figure 2. Effects of downregulation of SBP1 on cell proliferation, apoptosis, and GPX1 activity. A, cell proliferation was detected by CCK-8 assay. When both SBP1-siRNA and the control group were cultured under normal conditions, the proliferation rate of the control group was higher than that of the SBP1-siRNA group ($P < 0.05$). However, when both groups were treated with 100 μmol/L hydrogen peroxide, the cell proliferation in the control group was significantly suppressed after 48 hours whereas the SBP1-siRNA group maintained most of its proliferative ability ($P < 0.0001$). B, cell apoptosis was analyzed by flow cytometry. Fluorescein isothiocyanate (FITC)-labeled Annexin V and fluorescent dye propidium iodide (PI) were used to stain cells. No obvious differences were shown between the SBP1-siRNA group and the control group when cultured using normal medium. A significant decrease in the apoptosis rate of the SBP1-siRNA group was observed when cells were treated with hydrogen peroxide (300 μmol/L) for 12 hours. C, Western blot analysis showed the different HIF-1α and GPX1 expression levels in SMMC7721 cells following SBP1-siRNA transfection and different hydrogen peroxide treatment. GAPDH was used as a loading control. D, GPX1 activity of the SBP1-siRNA group was significantly higher than that of the control groups ($P < 0.001$), and a slight increase could be observed between the hydrogen peroxide–treated and -untreated groups. All experiments were repeated at least 3 times.

and the newly formed structure were colocalized, indicating that the 2 proteins might bind to each other under oxidative stress (Fig. 3B). After silencing SBP1, no specific association between SBP1 and GPX1 could be observed, but the GPX1 nuclear bodies remained (Fig. 4). The physiologic and pathologic implications behind this phenomenon would be discussed later.

Decreased SBP1 and increased GPX1 activity correlate with vascular invasion in HCC patients

We further validated our *in vitro* findings using clinical samples obtained from patients with HCC (Fig. 5A, Fig. 5B). We observed that samples with low expression of SBP1 had relatively high GPX1 activities whereas samples with high expression of SBP1 had limited GPX1 activities. Overall, the

Published OnlineFirst April 18, 2012; DOI:10.1158/1078-0432.CCR-12-0183

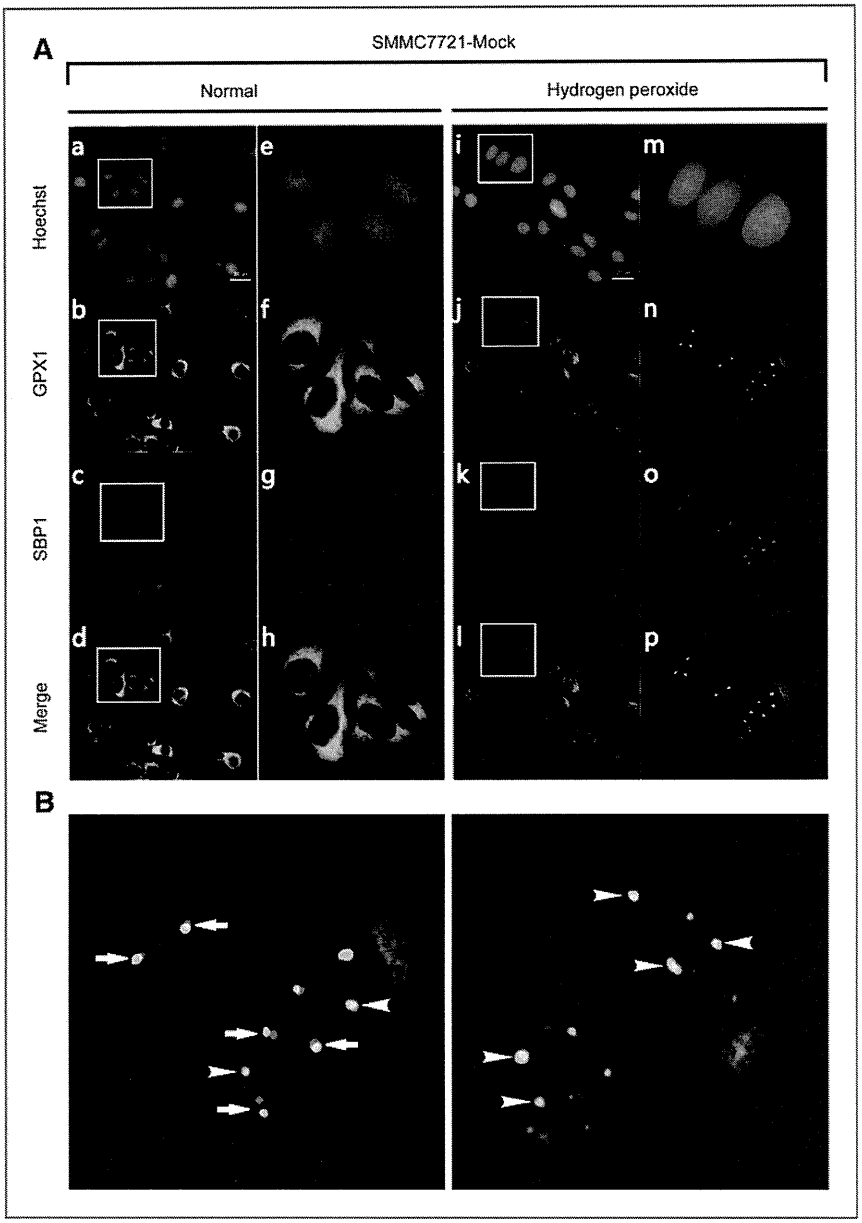

Figure 3. Immunofluorescence images of SBP1 and GPX1 in SMMC7721-Mock cells. A, SMMC7721 cells were stained with anti-SBP1 monoclonal antibody (red) and anti-GPX1 polyclonal antibody (green). a–h, cells were cultured without hydrogen peroxide treatment, and GPX1 localized exclusively in the cytoplasm (b, f) whereas SBP1 could be found both in the cytoplasm and the nucleus (c, g). i–p, cells were treated with hydrogen peroxide (50 μmol/L) for 12 hours before fixation. Images showed that both GPX1 and SBP1 had established specific nuclear bodies (j, k, n, o), and most of the GPX1 nuclear bodies were colocalized with SBP1 bodies (l, p). B, two high magnification images are presented here to show the details of the colocalization of SBP1 and GPX1 nuclear bodies. Some had already merged together (indicated by arrowheads) whereas others were still in the process of colocalization (indicated by arrows). We carried out the experiment at least 3 times and obtained similar results.

vascular invasion group had a lower SBP1 expression and relatively higher GPX1 activity, particularly in patients with HCC with macrovascular invasion, compared with those of the nonvascular invasion group (Supplementary Table S1).

Immunohistochemical characteristics

Representative photomicrographs of tumor tissues showing the various staining patterns are presented in Fig. 6A. In tumor tissues, we observed 26.01% (84 of 323) with scores of 0, 38.08% (123 of 323) with scores of +, 22.60% (73 of 323) with scores of ++, and 13.31% (43 of 323) with scores of +++. Of the 84 patients with scores of 0 in the tumor tissues, 78.57% (66 of 84) experienced recurrent disease, as did 65.86% (81 of 123), 52.05% (38 of 73) and 53.49% (23 of 43) of patients with scores of +, ++, and +++, respectively. With Kaplan–Meier estimates and log-rank tests considering the intensities of staining in tumor tissues, we found that the cutoff score of ++ was suitable to be the criterion (Supplementary Fig. S1); thus, we defined the samples with scores of 0 and + as negative and the samples with ++ and +++ as positive. According to the criterion

Published OnlineFirst April 18, 2012; DOI:10.1158/1078-0432.CCR-12-0183

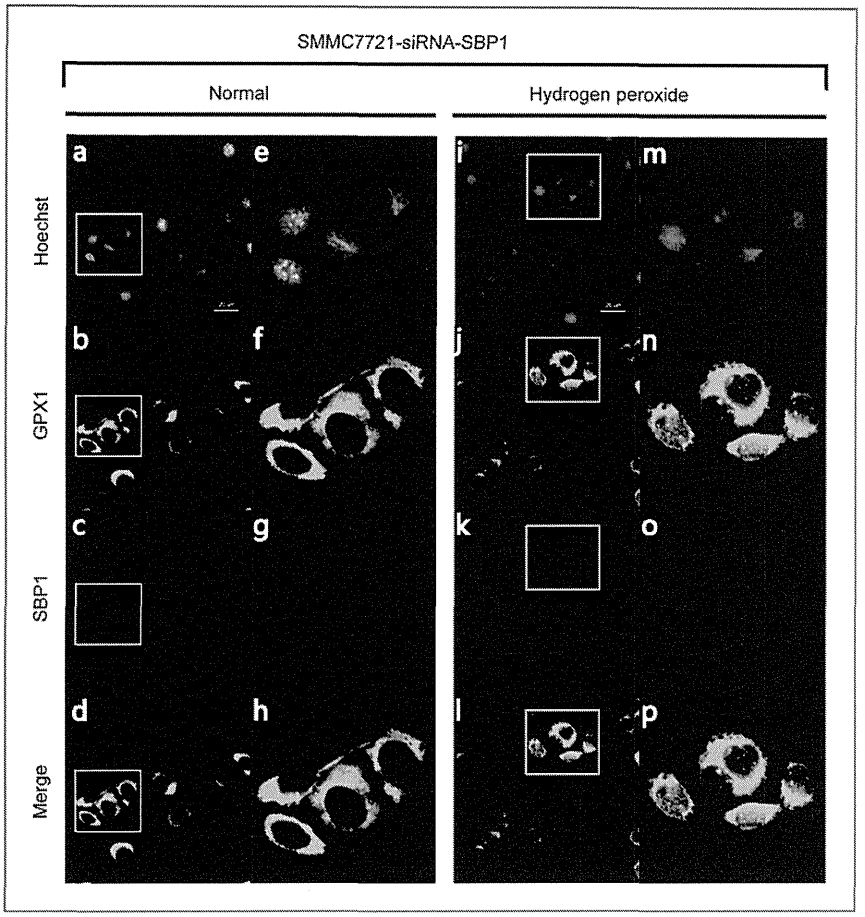

Figure 4. Images of SBP1 and GPX1 in SMMC7721-siRNA-SBP1 cells. SMMC7721-siRNA-SBP1 cells were stained with anti-SBP1 monoclonal antibody (red) and anti-GPX1 polyclonal antibody (green). a–h, cells were cultured under normal conditions. i–p, cells were treated with hydrogen peroxide (50 μmol/L) for 12 hours before fixation. SBP1 expression was downregulated to a minimal level by siRNA treatment (c, g, k, o) whereas GPX1 expression was unaffected (b, f, j, n). Similarly, GPX1 nuclear bodies were formed under hydrogen peroxide treatment (j, n) but were not colocalized with SBP1 bodies (l, p). We carried out the experiments at least 3 times and obtained similar results.

used, 64.09% (207 of 323) of the patients with HCC were negative for expression of SBP1.

As showed in Supplementary Table S2, negative SBP1 expression in tumor tissues was significantly correlated with patient age ($P = 0.045$), α-fetoprotein ($P < 0.001$), tumor size ($P = 0.005$), tumor number ($P = 0.019$), tumor encapsulation ($P = 0.034$), vascular invasion ($P < 0.001$), and recurrence ($P < 0.001$). Levels of SBP1 expression in tumor tissues were significantly different among patient groups according to the degree of vascular invasion ($P < 0.001$).

SBP1 expression in tumor tissue and prognosis

In the univariate analysis, patient sex, serum albumin (ALB), tumor differentiation, tumor encapsulation, tumor size, tumor number, and vascular invasion were associated with OS; patient sex, serum alanine transaminase (ALT), tumor encapsulation, tumor size, and vascular invasion were associated with cumulative recurrence (Supplementary Table S3). In the multivariate analysis, patient sex, serum ALB, tumor differentiation, tumor encapsulation, tumor size, and vascular invasion were associated with OS; patient sex, serum ALT, tumor encapsulation, tumor size, and vascular invasion were associated with cumulative recurrence (Supplemental Table S4). Univariate and multivariate analyses showed that SBP1 expression in tumor cells was an independent risk factor for both OS ($P < 0.001$) and recurrence ($P < 0.001$).

On the basis of Kaplan–Meier survival curves, patients who were negative for expression of SBP1 in tumor tissues experienced shorter OS periods ($P < 0.001$) and higher recurrence rates ($P < 0.001$; Fig. 6B). We investigated the predictive value of SBP1 in HCC. Of the patients with negative SBP1 expression in their tumor tissues, 69.08% (143 of 207) had recurred, and 114 patients of these patients experienced recurrence within 2 years. In patients with positive SBP1 expression in tumor cells, the recurrence rate was only 50.86% (59 of 116), and 28.45% (33 of 116) of these patients experienced recurrence within 2 years. Kaplan–Meier survival curves revealed that SBP1 was a significant prognostic factor for OS and early recurrence in HCC.

We further stratified patients by Milan criteria and investigated the predictive value of SBP1 in different

Published OnlineFirst April 18, 2012; DOI:10.1158/1078-0432.CCR-12-0183

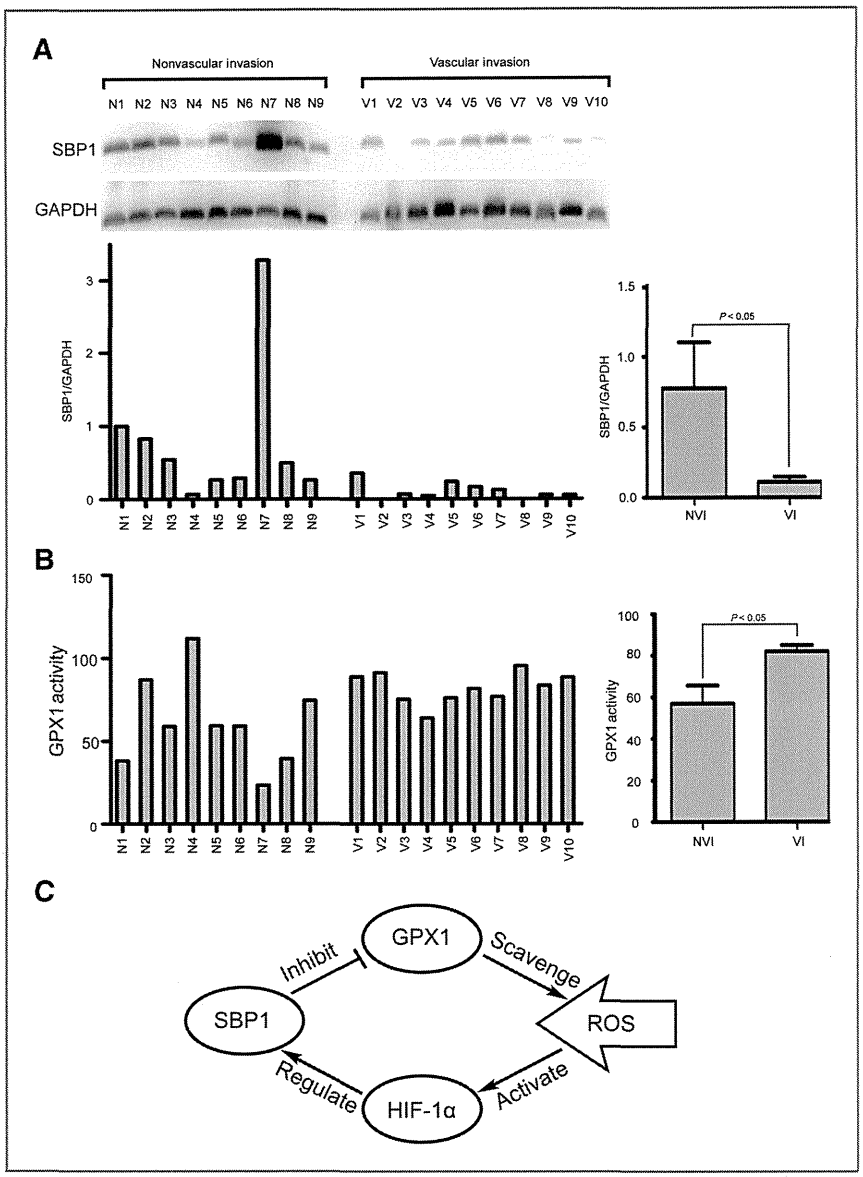

Figure 5. Relationships among clinical tumor characteristics, SBP1 and GPX1. Nineteen samples surgically removed from patients with HCC were included in this trial. All samples were preserved in liquid nitrogen immediately after resection and were analyzed within 2 weeks. These 19 samples were divided into 2 groups (N1–N9, V1–V10) based on their tumor characteristics (Supplementary Table S1). A, the vascular invasive group (VI group) had consistently low expressions of SBP1 whereas the nonvascular invasive group (NVI group) had higher and varied expressions of SBP1. B, GPX1 activity of the VI group was consistently at a relatively high level whereas the NVI group also exhibited a varied and lower activity of GPX1. Samples with high expression of SBP1 had limited GPX1 activity (e.g., N1, N7, and N8) whereas samples with lower expression of SBP1 had relatively high GPX1 activity (e.g., N4, N9, V2, and V8). C, the possible relationship among SBP1, GPX1, HIF-1α, and ROS.

subpopulations. Interestingly, in the subpopulation of patients with HCC within the Milan criteria, Kaplan–Meier survival curves revealed that SBP1 was not an effective prognostic factor for OS ($P > 0.05$) but was for early recurrence ($P = 0.039$; Fig. 6C). However, in the subpopulation of patients with HCC beyond Milan criteria with positive SBP1 expression in tumor tissues, only 35.85% (19 of 53) of patients recurred within 2 years. The results indicated that even patients beyond Milan criteria could experience a relatively longer OS and lower recurrence rate with tumors positive for SBP1 expression ($P < 0.001$). The prognostic significance of SBP1 was retained in the subpopulation of patients with HCC beyond Milan criteria (Fig. 6D).

Discussion

As shown by our study, most HCC cell lines have a minimal SBP1 expression, with the exception of SMMC7721. Compared with other HCC cell lines, SMMC7721 has a low metastatic potential (24). In our study, the migration potential of SMMC7721 cells was inhibited by the expression of SBP1. However, SBP1 only exhibited its impact on cancer cell proliferation and apoptosis following treatment with hydrogen peroxide; these results indicated that SBP1 might exert its tumor suppressive power through modulation of the tumor redox microenvironment.

Published OnlineFirst April 18, 2012; DOI:10.1158/1078-0432.CCR-12-0183

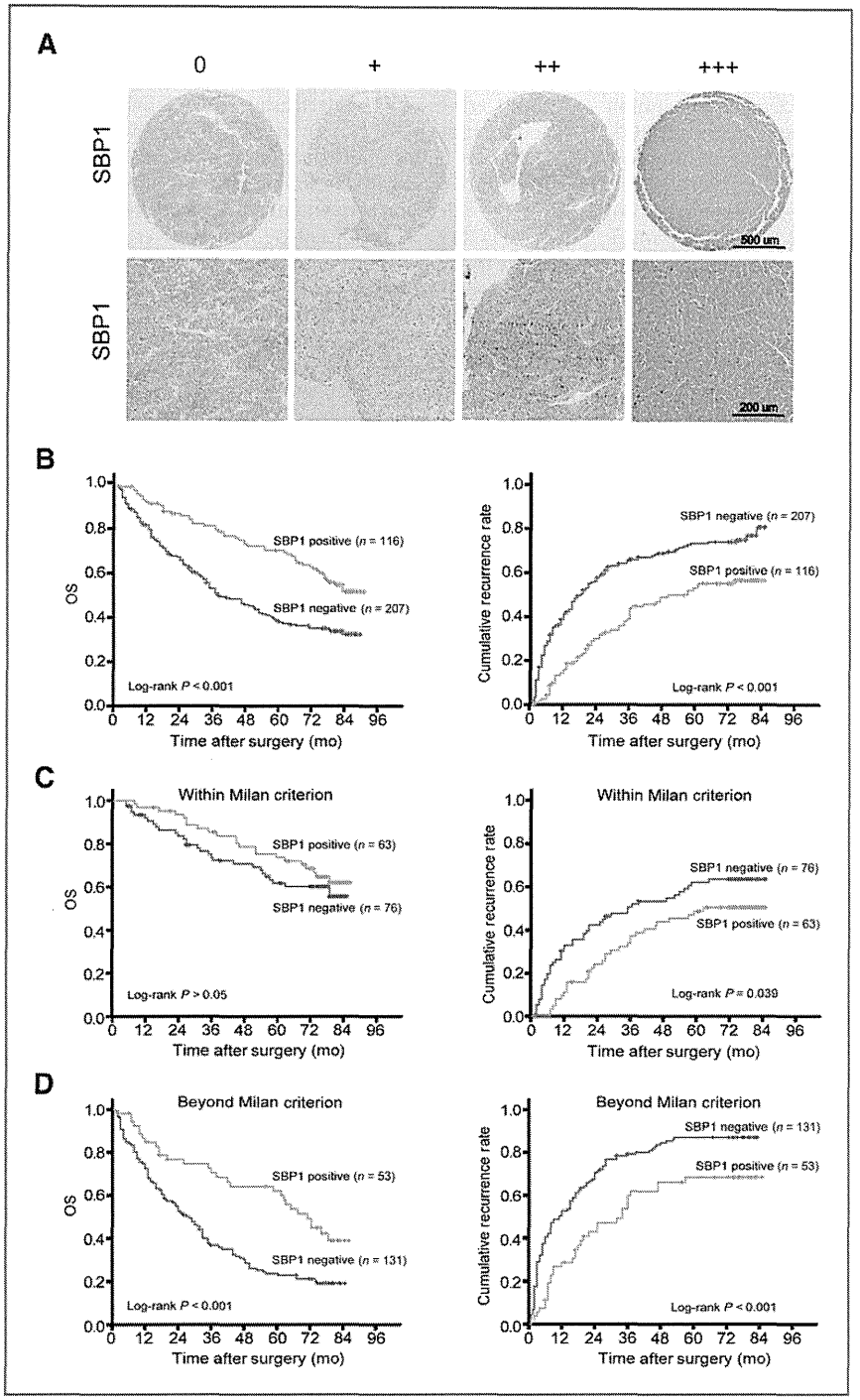

Figure 6. SBP1 expression in tumor tissue and prognosis. Three hundred and twenty-three HCC samples surgically removed between 2003 and 2004 were included here. A, representative photomicrographs of tumor tissues showing the different staining patterns are presented here and are graded from 0 to +++. B, Kaplan–Meier survival curves showed that patients with negative expression of SBP1 in tumor cells experienced shorter OS periods ($P < 0.001$) and higher recurrence rates ($P < 0.001$) than patients with positive expression of SBP1. C, Kaplan–Meier survival curves revealed that SBP1 was not a significant prognostic factor for OS in HCC within Milan criteria ($P > 0.05$) but was significant for the recurrence in these patients ($P = 0.039$). D, in the subpopulation of patients with HCC beyond Milan criteria, SBP1 was a significant prognostic factor for OS ($P < 0.001$) and recurrence ($P < 0.001$).

GPX1 is the most important antioxidant enzyme that protects cells from ROS such as hydrogen peroxide and singlet oxygen species (29). ROS have the potential to create oxidative stress within cells that causes DNA damage, protein degradation, peroxidation of lipids, and finally leads to cell transformation or death based on ROS concentration (30). It is a well-documented fact that cancer cells are under high levels of oxidative stress compared with normal cells